Iraqi Journal of Physics, 2016 *Vol.14, No.30, PP. 42-50*

Study of charge density distributions, elastic charge form factors and root-mean square radii for ^{4}He, ^{12}C and ^{16}O nuclei using Woods-Saxon and harmonic-oscillator potentials

Arkan R. Ridha

Department of Physics, College of Science, University of Baghdad, Baghdad, Iraq

E-mail: arkan_rifaah@yahoo.com

Abstract

The nuclear charge density distributions, form factors and corresponding proton, charge, neutron, and matter root mean square radii for stable ^{4}He, ^{12}C, and ^{16}O nuclei have been calculated using single-particle radial wave functions of Woods-Saxon potential and harmonic-oscillator potential for comparison. The calculations for the ground charge density distributions using the Woods-Saxon potential show good agreement with experimental data for ^{4}He nucleus while the results for ^{12}C and ^{16}O nuclei are better in harmonic-oscillator potential. The calculated elastic charge form factors in Woods-Saxon potential are better than the results of harmonic-oscillator potential. Finally, the calculated root mean square radii usingWoods-Saxon potentials how overestimation in comparison with experimental data on contrary to the results of harmonic-oscillator potential.

Key words

Stable nuclei, ground density distribution, elastic form factor, root-mean-square radii, Woods-Saxon potential.

Article info.

Received: Dec. 2015
Accepted: Feb. 2016
Published: Sep. 2016

دراسة توزيعات الكثافة الشحنية وعوامل التشكل الشحنية المرنة وأنصاف الأقطار للنوى ^{4}He و ^{12}C و ^{16}O باستخدام جهد ودز- ساكسون وجهد المتذبذب التوافقي

أركان رفعه رضا

قسم الفيزياء، كلية العلوم، جامعة بغداد، بغداد، العراق

الخلاصة

تمت دراسة توزيعات الكثافة الشحنية النووية وعوامل التشكل المرنة بالإضافة إلى أنصاف الأقطار البروتونية والشحنية والنيوترونية والكتلية للنوى المستقرة (^{4}He و ^{12}C و ^{16}O) باستخدام الدوال الموجية القطرية لجهد ودز- ساكسون بالأضافة الى جهد المتذبذب-التوافقي لغرض المقارنة. أظهرت نتائج توزيع الكثافة الشحنية المحسوبة بجهد ودز - ساكسون تطابق جيد بالنسبة لنواة ^{4}He مع القيم العملية بينما كانت نتائج جهد المتذبذب التوافقي أفضل بالنسبة للنواتين ^{12}C و^{16}O. أما نتائج عوامل التشكل الشحنية المرنة للحالة الأرضية المحسوبة بجهد ودز- ساكسون فكانت أفضل من نتائج جهد المتذبذب التوافقي. وأخيرا أظهرت نتائج أنصاف الأقطار النووية المحسوبة بواسطة جهد ودز- ساكسون تقدير زائد عن تلكم المحسوبة بواسطة جهد المتذبذب-التوافقي عند مقارنة نتائج كلا الجهدين مع النتائج العملية.

Introduction

The radial distributions and sizes of nuclear matter and charges are basic properties of nuclei. They are important to test the validity of the nuclear single-particle wave functions used especially in density folding models [1]. The harmonic-oscillator (HO) potential is not accurate to describe the nuclear central confining potential because the potential continues to give a contribution even for much larger *r* (distance from the center of nucleus) and does not become zero, besides the radial wave functions obtained from HO have a Gaussian fall-off behavior at large *r* which does not reproduce the correct exponential tail. In this field, Elton and Swift [2] firstly reproduced single-particle radial wave functions in a parameterized single-particle local Woods-Saxon (WS) potential and adjusted the parameters so as to fit the shape of the wave functions to elastic electron scattering data and the eigen-energies to the proton separation energies in the $1p$ and $2s-1d$ shell nuclei. Gibson et al. [3] studied the ground state of the ^{4}He nucleus using the single-particle phenomenological model. Wave functions were regenerated from a WS potential whose parameters are chosen to regenerate the correct neutron separation energy. The proton separation energy and electron scattering form factors were then calculated. Gamba et al. [4] calculated the parameters of a WS potential well for ten p-shell nuclei by fitting the electron scattering form factors and single-particle separation energies. Brown et al. [5] described a new method for calculating nuclear charge and matter distributions which is complementary to the Hartree-Fock method taking into account shell model configuration mixing but it is only semi-self-consistent because the potential was allowed to vary linearly with the density. The method was applied to the core nuclei ^{16}O and ^{40}Ca. Lojewski et al. [6] used realistic single-particle WS potential to evaluate the mean-square charge radii for even-even nuclei. Lojewski and Dudek [7] evaluated the proton and neutron separation energies and mean square charge radii within the WS plus BCS model for even-even nuclei with $40 \leq A \leq 256$. In [8] some properties of the solutions to the Dirac equations with WS potential were studied, the results obtained for spherical nuclei were compared to those of the relativistic mean field theory. In [9] the single-particle energies and wave functions of an axially two-center WS potential were computed. The spin-orbit interaction was included in the Hamiltonian. In [10] the WS potential has been considered to compute the eigenvalues by using Numerov method for a Sturm-Liouville problem. In [11] the Schrödinger equation has been solved by using the Pekeris approximation, for the nuclear deformed WS potential within the framework of the asymptotic iteration method. The energy levels have been worked out and the corresponding normalized eigen functions have been obtained in terms of hypergeometric function.

The aim of the present work is to calculate ground state matter, proton, charge densities, and neutron root mean square (rms) radii, charge density distributions (CDD), elastic charge form factors for stable ^{4}He, ^{12}C, and ^{16}O nuclei using the radial wave functions of WS and HO potentials.

Theoretical formulations

The Schrödinger equation for the single-particle radial wave function can be written as [5]:

$$\left(\frac{\hbar^2}{2\mu}\frac{d^2}{dr^2} - v(r) - \frac{l(l+1)\hbar^2}{2\mu r^2} + \varepsilon_{nlj}\right) R_{nlj}(r) = 0 \quad (1)$$

where $\mu = m(A-1)/A$ is the reduced mass of the core $(A-1)$ and single nucleon, m is the nucleon mass, A is the atomic mass, ε_{nlj} is the single nucleon separation energy, $R_{nlj}(r)$is the radial eigenfunction of WS potential, n,l, and j are the principal, orbital angular, and total quantum numbers.

For the local potential $v(r)$, the WS shape is used in the compact form shown below [2,4]:

$$v(r) = v_{cent}(r) + v_{s.o.}(r) + v_c(r) \quad (2)$$

where

$$v_{cent}(r) = \frac{-U_0}{\left(1+e^{\left(\frac{r-R}{a}\right)}\right)} \quad (3)$$

represents the central part of $v(r)$, U_0 is the strength or depth of central potential, the $a_0$is the diffuseness and $R = r_0(A-1)^{1/3}$ is the radius parameter.

$$v_{s.o.}(r) = -2\left(\frac{\hbar}{m_\pi c}\right)^2 \frac{U_{s.o.}}{r}\frac{d}{dr}\frac{1}{\left(1+e^{\left(\frac{1-R_{s.o.}}{a_{s.o.}}\right)}\right)}\langle \hat{l}.\hat{\sigma}\rangle = 2\left(\frac{\hbar}{m_\pi c}\right)^2 \frac{U_{s.o.}}{r}\frac{e^{\left(\frac{1-R_{s.o.}}{a_{s.o.}}\right)}}{\left(1+e^{\left(\frac{1-R_{s.o.}}{a_{s.o.}}\right)}\right)^2}\langle \hat{l}.\hat{\sigma}\rangle \quad (4)$$

where $\left(\frac{\hbar c}{m_\pi c^2}\right)^2 = 1.99901\, fm^2$
with $m_\pi c^2 = 139.5669\, MeV$
and $\hbar c$ =197.32858$MeV.fm^2$.

$$\langle \hat{l}.\hat{\sigma}\rangle = \begin{cases} -\frac{1}{2}(l+1) & for\; j = l-\frac{1}{2} \\ \frac{1}{2}l & for\; j = l+\frac{1}{2} \end{cases}$$

Eq. (4) represents the spin-orbit part of $v(r)$, m_π is the pion mass,$U_{s.o.}$ is the strength or depth of spin-orbit potential, $a_{s.o.}$is the diffuseness of spin-orbit part, $R_{s.o.} = r_{s.o.}(A-1)^{\frac{1}{3}}$ is the radius parameter of spin-orbit and$\hat{l}$ and $\hat{\sigma}$ are the angular momentum and the spin operators respectively.

Finally, in Eq. (2) $v_c(r)$ indicates the Coulomb potential generated by a homogeneous charged sphere and can be written as [12]:

$$v_C(r) = \begin{cases} (Z-1)\frac{e^2}{r} & if\; r > R \\ \frac{(Z-1)e^2}{2R}\left[3-\frac{r^2}{R^2}\right] & if\; r < R \end{cases}, \quad (5)$$

for protons and $v_C(r) = 0$ for neutrons, with$e^2 = 1.44\, MeV.fm$. Therefore, Eq. (2) can be written as:

$$v(r) = \frac{-U_0}{\left(1+e^{\left(\frac{r-R}{a}\right)}\right)} - \left(\frac{\hbar}{m_\pi}\right)^2 \frac{1}{r}\frac{U_{S.O.}}{a_{S.O.}}\frac{e^{\left(\frac{r-R_{S.O.}}{a_{S.O.}}\right)}}{\left(1+e^{\left(\frac{r-R_{S.O.}}{a_{S.O.}}\right)}\right)^2}\langle \hat{l}.\hat{\sigma}\rangle + v_C(r) \quad (6)$$

The point density distributions of neutrons, protons, and matter can be written respectively as [13]:

$$\rho_{n,p\; or\; m}(r) = \frac{1}{4\pi}\sum_{nlj} X^{nlj}_{n,p\; or\; m}\left|R_{nlj}(r)\right|^2 \quad (7)$$

where $X^{nlj}_{n,p\; or\; m}$represents the number of neutrons, protons, or nucleons in the *nlj*-subshell. It is worth mentioning that the summation in Eq. (7) spans all occupied orbits.

In order to compare the calculated point proton density distributions with the experimental densities, the finite proton size is required to be included. The charge density distribution $\rho_{ch}(r)$(CDD) is obtained by folding the proton density ρ_{pr} into the distribution of the point proton density in Eq. (7)as follows [14]:

$$\rho_{ch}(r) = \int \rho_p(r)\rho_{pr}(\mathbf{r}-\mathbf{r}')d\mathbf{r}' \quad (8)$$

If $\rho_p(\vec{r})$is taken to have a Gaussian form, then

$$\rho_{pr}(r) = \frac{1}{\left(\sqrt{\pi}a_{pr}\right)^3} e^{\left(\frac{-r^2}{a_{pr}^2}\right)} \quad (9)$$

where $a_{pr} = 0.65\, fm$. Such value of a_{pr} reproduces the experimental charge rms radius of the proton, $\langle r^2\rangle^{1/2}_{pr} = \left(\frac{3}{2}\right)^{1/2} a_{pr} \approx 0.8\, fm$.

The rms radii of neutron, proton, charge and matter can be directly deduced from their density distributions [14] as follows:

$$\langle r^2\rangle^{1/2}_{n,p,ch,m} = \sqrt{\frac{4\pi}{X}\int_0^\infty \rho_{n,p,ch,m}(r) r^2 dr} \quad (10)$$

where X in Eq. (10) denotes N(number of neutrons), Z (atomic number which is the same for proton and charge) and A, respectively.

In the first Born approximation the elastic neutron, proton, charge and matter form factors are Fourier transforms of their corresponding density distributions [14]:

$$F_{n,p,ch,m}(q) = \frac{4\pi}{qX}\int_0^\infty \rho_{n,p,ch,m}(r)\sin(qr)\, r dr \quad (11)$$

where X takes the same definition in Eq. (10).

Results and discussion

The nuclear shell model is used to calculate CDDs, form factors and corresponding proton, charge, neutron, and matter rms radii for ^{4}He, ^{12}C, and ^{16}O nuclei. The WS potential is used to regenerate the radial wave functions and experimental single nucleon (proton/neutron) separation energies. The WS parameters U_0, $U_{s.o.}$, a_0, $a_{s.o.}$, r_0, $r_{S.O.}$, and R_C are adjusted so as to reproduce the experimental single nucleon separation energies in different subshells for nuclei under study.

For ^{4}He, ^{12}C, and ^{16}O nnuclei, the parameters chosen for WS potential are shown in Table 1. The results for the calculated single nucleon separation energies are shown in Table 2.

Table 1: The WS parameters U_0, $U_{s.o.}$, a_0, $a_{s.o.}$, r_0, $r_{S.O.}$, and R_C for ^{4}He, ^{12}C, and ^{16}O nuclei.

^{4}He	nl_j	$U_0(MeV)$	$U_{s.o.}(MeV)$	$a_0(fm)$	$a_{s.o.}(fm)$	$r_0(fm)$	$r_{S.O.}(fm)$	$R_C(fm)$
n	$1s_{1/2}$	56.70	15.0	0.01	0.01	1.350	1.350	0.0
p	$1s_{1/2}$	56.53	15.0	0.01	0.01	1.333	1.333	1.333
^{12}C								
n	$1s_{1/2}$	59.76	15.0	0.527	0.527	1.236	1.236	0.0
	$1p_{3/2}$	59.10	15.0	0.527	0.527	1.236	1.236	0.0
p	$1s_{1/2}$	60.05	15.0	0.518	0.518	1.230	1.230	1.23
	$1p_{3/2}$	59.21	15.0	0.518	0.518	1.230	1.230	1.23
^{16}O								
n	$1s_{1/2}$	51.08268	15.0	0.5	0.5	1.375	1.375	0.0
	$1p_{3/2}$	50.18035	15.0	0.5	0.5	1.375	1.375	0.0
	$1p_{1/2}$	52.43502	15.0	0.5	0.5	1.375	1.375	0.0
p	$1s_{1/2}$	50.66585	15.0	0.5	0.5	1.375	1.375	1.375
	$1p_{3/2}$	50.35321	15.0	0.5	0.5	1.375	1.375	1.375
	$1p_{1/2}$	52.48221	15.0	0.5	0.5	1.375	1.375	1.375

Table 2: The calculated (E_{cal}) and experimental (E_{exp}) single nucleon (proton/neutron) separation energies for different subshells for ^{4}He, ^{12}C, and ^{16}O nuclei

^{4}He	nl_j	$E_{cal} = E_{exp.}(MeV)$ [15]
n	$1s_{1/2}$	20.5776
p	$1s_{1/2}$	19.8139
^{12}C		
n	$1s_{1/2}$	34.04
	$1p_{3/2}$	18.72
p	$1s_{1/2}$	30.9
	$1p_{3/2}$	15.75
^{16}O		
n	$1s_{1/2}$	34.03
	$1p_{3/2}$	21.81
	$1p_{1/2}$	15.65
p	$1s_{1/2}$	29.81
	$1p_{3/2}$	18.44
	$1p_{1/2}$	12.11

The results of the calculated charge, matter, proton, and neutron rms radii for ^{4}He, ^{12}C, and ^{16}O nuclei are presented in Table 3. For ^{4}He nucleus, the results in WS potential for the charge and matter rms radii showed overestimation in comparison with experimental data on contrary to the results of HO potential which can reproduce such experimental data. Regarding the calculated proton and neutron rms radii in both potentials, there is appreciable variation between the results of both potentials. Unfortunately, there are no available experimental data to compare with. For ^{12}C nucleus, the calculations in both WS and HO potentials for the calculated charge and matter rms radii showed very good agreement with experimental data. For the calculated proton rms radii, the results of both potentials are almost equal on contrary to the results of the calculated neutron rms radii which showed large deviation for both potentials. In ^{16}O nucleus, the calculated charge rms radius in WS and HO potentials are both in excellent agreement with experimental data, while the results for the calculated matter rms radii showed slight overestimation in WS potential in comparison with experimental data on contrary to the results of HO potential which agree with the experimental data. The calculated proton rms radii in WS and HO potential are also almost the same. Appreciable deviation is observed for the calculated neutron rms radii in both potentials.

Table 3: The calculated charge $\langle r^2\rangle_{ch}^{1/2}$, matter $\langle r^2\rangle_{m}^{1/2}$, proton $\langle r^2\rangle_{p}^{1/2}$, and neutron $\langle r^2\rangle_{n}^{1/2}$ rms radii in Fermi's (fm) units with corresponding available experimental data.

nucleus	Calculated $\langle r^2\rangle_{ch}^{1/2}$	Exp. $\langle r^2\rangle_{ch}^{1/2}$ [16]	Calculated $\langle r^2\rangle_{m}^{1/2}$	Exp. $\langle r^2\rangle_{m}^{1/2}$ [17]	Calculated $\langle r^2\rangle_{p}^{1/2}$	Calculated $\langle r^2\rangle_{n}^{1/2}$
^{4}He	WS: 1.885	1.676(8)	WS: 1.709	1.57(4)	WS: 1.714	WS: 1.704
	HO: 1.676		HO: 1.570		HO: 1.475	HO: 1.659
^{12}C	WS: 2.464	2.464(12)	WS: 2.326	2.31(2)	WS: 2.336	WS: 2.316
	HO: 2.464		HO: 2.310		HO: 2.332	HO: 2.287
^{16}O	WS: 2.737	2.737(8)	WS: 2.606	2.54(2)	WS: 2.623	WS: 2.589
	HO: 2.737		HO: 2.54		HO: 2.619	HO: 2.458

The calculated charge density distributions are depicted in Fig. 1 for ^{4}He (a), ^{12}C (b), and ^{16}O (c) nuclei in WS (solid curve) and HO (dashed curve) potentials. For ^{4}He nucleus, it is clear from Fig. 1 (a) that the result from WS is better than the result from HO potential which showed a large deviation from experimental data at central region. In Fig. 1 (b), the calculated CDDs for ^{12}C nucleus in both WS and HO potentials are depicted. It is clear that the results of WS and HO potentials are almost the same in central region with slight deviation upwards of the WS potential from experimental data. Finally, the results of the calculated CDDs in WS and HO potentials are shown in Fig.1(c). It is obvious that the result of HO potential is better than WS potential in central region on contrary to result of HO potential which showed an appreciable underestimation in the central region with behavior going well with experimental data in central region.

The calculated charge form factors are illustrated in Fig.2 for ^{4}He (a), ^{12}C (b), and ^{16}O (c) nuclei in WS (solid curve) and HO (dashed curve) potentials. For ^{4}He nucleus (Fig. 2(a)), it is clear that the result of WS is better than the result of HO potential which completely failed to reproduce the first diffraction minimum in comparison with experimental data. For ^{12}C nucleus (Fig.2 (a)), the result of WS potential predicts the existence of second diffraction minimum. The result for HO potential is slightly better than the result of WS potential for all q regions. Finally, in Fig. 2(c), the charge form factor for ^{16}O nucleus is illustrated. The results in HO potential failed to reproduce the second diffraction minimum while the result of WS potential is very good at low and medium q regions. At high q region, the result for WS potential slightly overestimates the position of second diffraction minimum by roughly $0.1\ fm^{-1}$, and underestimates the calculated charge form factors downwards at second diffraction minimum and beyond.

Conclusions

The nuclear charge density distributions (CDD), form factors, and corresponding proton, charge, neutron, and matter rms radii besides single nucleon binding energies for stable ^{4}He, ^{12}C, and ^{16}O are calculated in both Woods-Saxon (WS) and harmonic-oscillator (HO) potentials. The results showed an overestimation in the calculated charge, matter, proton, and neutron rms radii in WS potential for ^{4}He nucleus in comparison with available experimental data on contrary to the results of HO potential which easily reproduce the available experimental data. For ^{12}C nucleus, the charge, matter, and proton rms radii are almost well generated in both WS and HO potential but with appreciable deviation for neutron rms radii for both potentials. For ^{16}O nucleus, the results of the calculated charge and proton rms radii are roughly the same. The deviation appreciably noticed in matter and neutron rms radii for both potentials where the result for HO potential is better than the result for WS potential in comparison both with available experimental data. In general, there is an overestimation in the calculated rms radii in WS potential. For the calculated CDDs, the results for WS potential in ^{4}He nucleus are much better than results for HO potential. For ^{16}O nucleus, the behaviors in both potentials are the same but in HO potential is better. For ^{12}C nucleus, the results in HO potential are much better than results of WS potential. Regarding the calculated charge form factors, for ^{4}He nucleus, the results in WS potential is much better in HO potential which completely failed to predict the existence the first diffraction minimum. For ^{12}C nucleus, the results for both potentials are the same at all q regions with the difference that there is a second diffraction minimum predicted by WS potential. Finally, for ^{16}O nucleus, the results for WS potential are much better in comparison with experimental data than the results for HO potential which completely failed to reproduce the second diffraction minimum.

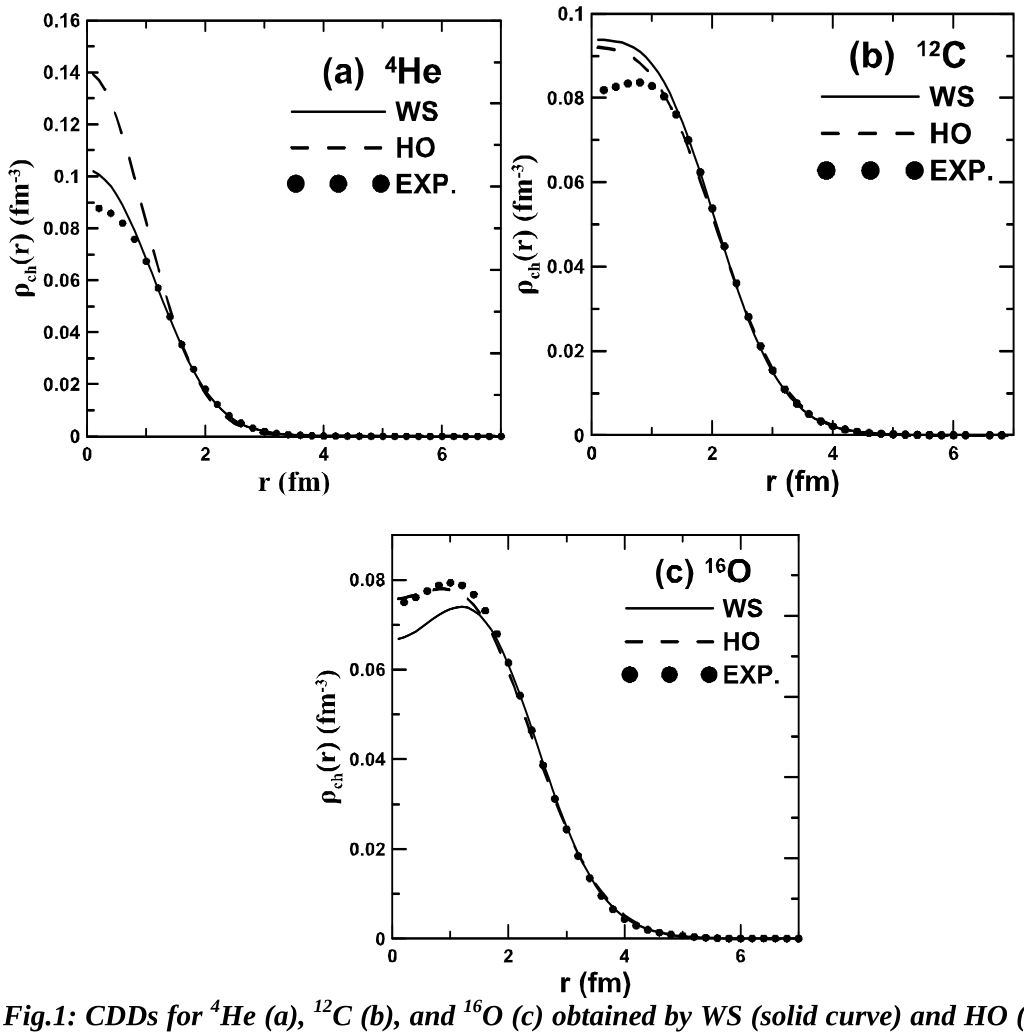

Fig.1: CDDs for ^{4}He (a), ^{12}C (b), and ^{16}O (c) obtained by WS (solid curve) and HO (dashed curve) potentials. The experimental data are denoted by filled dotted circles and taken from[16].

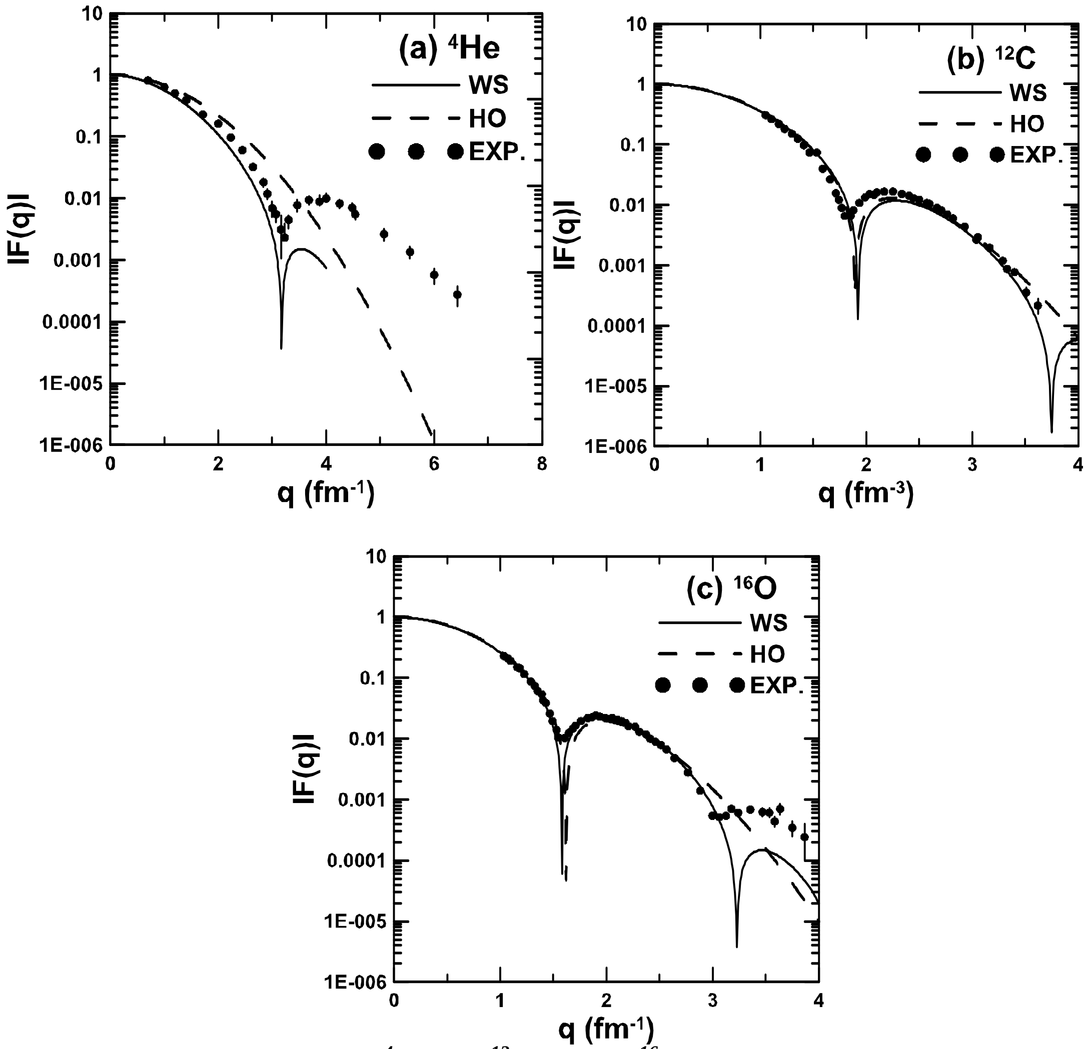

Fig. 2: Charge form factorsfor ^{4}He (a), ^{12}C (b) and ^{16}O (c) calculated by WS (solid curve) and HO (dashed curve) potentials. The experimental data are denoted by filled dotted circles and taken from [18, 19] for ^{4}He and [20] for both ^{12}C and ^{16}O nuclei.

References

[1] G. R.Satchler and W. G. Love. Physics Reports, 55 (1979) 183-254.
[2] L. R. B. Elton and A. Swift. Nuclear Physics, A94 (1967) 52-72.
[3] B. F. Gibson,A. Goldberg andM. S. Weiss. Nuclear Physics A, 111 (1968) 321-330.
[4] S. Gamba, G. Riccoand G. Rottigni. Nuclear Physics A213 (1973) 383-396.
[5] B. A. Brown, S. E. Massen and P. E. Hodgson. Journal of Physics G, 5 (1979) 1655-1698
[6] Z. Lojewski, B. Nerlo-Pomorska, K. Pomorski. Physical Review C, 51 (1995) 601-605.
[7] Z. Lojewski and J. Dudek. Acta Physica Polonica B 29 (1998) 407-417.
[8] Nicolas Schunck and Jerzy Dudek. Acta Physica Polonica B, 32 (2001) 1103-1106
[9] M. Mirea. Romanian Reports in Physics, 59 (2007) 523-531.
[10] A. H. Fatah. Adv. Theor. Appl. Mech. 5 (2012) 23-31.
[11] S. M. Ikhdair, B. J. Falaye, M. Hamzavi. Chin. Phys. Lett. 30 (2013) 020305 (1-5)
[12] Peter Ring and Peter Schuck, “The Nuclear Many-Body Problem”, Springer-Verlag (1981).
[13] A.N.Antonov, P.E.Hodgson and I.Zh.Petkov, “Nucleon Momentum and

Density Distributions in Nuclei", Clarendon Press, Oxford (1988).
[14] L. R. B. Elton, "Nuclear Sizes", Oxford University Press (1961).
[15] C. M. Lederer and Shirley V. S., "Table of Isotopes, 7^{th} ed.", John Wiley and Sons, New York, 1978.
[16] H.De Vries, C. W.De Jager, C.De Vries. Atomic Data and Nuclear Data Tables, 36 (1987) 495-536.
[17] A.Ozawa, T.Suzuki, I.Tanihata. Nuclear Physics A, 693 (2001) 32-62.
[18] R.Frosch. Phys. Lett. B 37 (1971) 140-142.
[19] R. G.Arnold, B. T.Chertok, S.Rock, W. P.Schütz, Z. M.Szalata, D.Day, J. S.McCarthy, F.Martin, B. A.Mecking, I.Sick, G.Tamas.Phys. Rev. Lett. 40 (1978) 1429- 1432.
[20] I.Sick and J. S. McCarthy. Nucl. Phys. A 150 (1970) 631-654.